RECENT MEASUREMENTS OF NUCLEON STRUCTURE FUNCTIONS FROM NEUTRINO SCATTERING

A. Para[*]

CERN, Geneva, Switzerland

Summary

New results from charged current neutrino inter-actions are compared with quark-parton model predictions. Data on scaling violation are reviewed. Tests of quantum chromodynamics are discussed.

Kinematics

Inclusive neutrino-nucleon "charged current" inter-action is represented by the diagram of Fig. 1. This reaction is described by three independent variables: p_ν, p_μ, p_N or any combination of them. Usually one uses:

$$s = (p_\nu + p_N)^2 = 2ME_\nu + M^2$$

$$Q^2 = -q^2 = -(p_\nu - p_\mu)^2$$

$$\nu = p_N\, q/M \qquad\qquad (1)$$

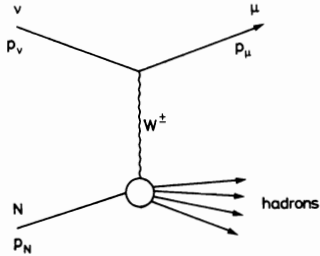$$x = Q^2/2M\nu$$

$$y = \nu/E_\nu \;.$$

Fig. 1 Deep inelastic lepton-nucleon scattering.

In experiments one measures muon momentum, angle and kinetic energy of hadrons. In terms of these quantities

$$E_\nu = E_{had} + E_\mu$$

$$Q^2 = 4E_\mu E_\nu \sin^2 \theta/2$$

$$\nu = E_{had} \qquad\qquad (2)$$

$$x = \frac{2E_\mu E_\nu \sin^2 \theta/2}{ME_{had}}$$

$$y = \frac{E_{had}}{E_{had} + E_\mu} \;.$$

Assuming V - A coupling, averaging over initial polarization, summing over final polarizations, and neglecting terms proportional to the leptons' masses, the most general form of the differential cross-section is

$$\frac{d\sigma^{\nu,\bar\nu}}{dxdy} = \frac{G^2 ME_\nu}{\pi} \left[\left(1 - y - \frac{Mxy}{2E_\nu}\right) F_2^{\nu,\bar\nu}(\nu,Q^2) + \frac{y^2}{2} 2xF_1^{\nu,\bar\nu}(\nu,Q^2) \pm y\left(1 - \frac{y}{2}\right) xF_3^{\nu,\bar\nu}(\nu,Q^2) \right] . \qquad (3)$$

The unknown functions $F_i(\nu,Q^2)$ describe the structure of the hadron vertex. They can be different for neutrinos and antineutrinos.

Quark-Parton Model

The quark parton model (QPM) tells us that in "deep inelastic" regions, i.e. for large Q^2 and ν, the nucleon can be described as a gas of point-like quasi-free partons-quarks. This means that a blow-up of the hadron vertex of Fig. 1 looks like Fig. 2, where ξ = the fraction of the nucleon momentum carried by the struck parton.
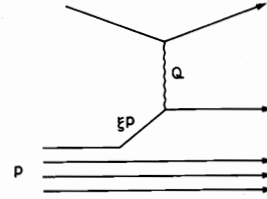

Fig. 2 The parton model for deep inelastic lepton-nucleon scattering.

Neglecting all masses - $\xi = x$. If we keep the nucleon mass

$$\xi = \frac{2x}{1 + \sqrt{1 + \dfrac{4M^2x^2}{Q^2}}} \;. \qquad (4)$$

As a consequence of spin ½ of partons we have the Callan-Gross relation

$$2xF_1(\nu,Q^2) = F_2(\nu,Q^2) \qquad (5)$$

(if partons have no transverse momentum).

Structure functions $F_i(\nu,Q^2)$ are predicted to scale, i.e.

$$F_i(\nu,Q^2) \rightarrow F_i(Q^2/2M\nu) = F_i(x) \;,$$

as there is no intrinsic mass scale in this model. In addition we obtain simple interpretation of structure functions in terms of quark and antiquark distributions. For an isoscalar target

$$F_2^\nu(x) = F_2^{\bar\nu}(x) = q(x) + \bar q(x)$$

$$xF_3^\nu(x) = q(x) - \bar q(x) + 2s(x) - 2\bar c(x) \qquad (6)$$

$$xF_3^{\bar\nu}(x) = q(x) - \bar q(x) - 2\bar s(x) + 2c(x)$$

where

$$q(x) = u(x) + d(x) + s(x) + c(x)$$

$$\bar q(x) = \bar u(x) + \bar d(x) + \bar s(x) + \bar c(x) \;,$$

---

[*] On leave of absence from Warsaw University.

u(x), ... being the momentum distribution of different flavours in the proton [one assumes $u_p(x) = d_n(x)$, $d_p(x) = u_n(x)$, $s_p(x) = s_n(x)$, $c_p(x) = c_n(x)$, ...]. From this one derives another prediction:

$$\int_0^1 F_3(x)\ dx = \int_0^1 \frac{1}{2}\left(F_3^\nu + F_3^{\bar\nu}\right)\ dx = 3 \ , \qquad (7)$$

known as the Llewellyn-Smith-Gross sum rule.

Neutrinos interact only with d and s quarks or $\bar{u}$ and $\bar{c}$ antiquarks, whereas antineutrinos see u and c quarks and $\bar{d}$ and $\bar{s}$ antiquarks. This fact allows us to study the distribution of different flavours inside the nucleon.

Scaling Violation and Quantum Chromodynamics

Some deviations from the predictions of QPM have been observed in deep inelastic electron and muon scattering. The most attractive explanation for this is offered by quantum chromodynamics (QCD). QCD says that quarks inside the nucleon are not free, but interact with each other via gluon emission. By increasing the Q^2 of our probe we are able to resolve quarks into the quark + gluon system or the gluon into the $q\bar{q}$ system (Fig. 3). As an effect the parton distribution becomes Q^2 dependent: it should shift towards low x as a consequence of gluon "gluestrahlung" as well as increase in the small x region, as it is fed by gluons "decaying" into $q\bar{q}$ pairs (Fig. 4). QCD is not able to calculate the shape of the quark and antiquark distribution, but it can predict their dependence on Q^2.
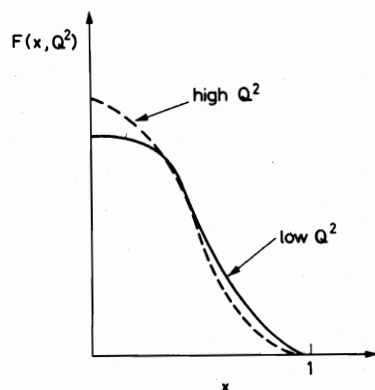
Measurements of the nucleon structure functions are certainly very interesting and important. They are the main source of information about nucleon constituents and their interactions, information which can be confronted with actual theories or models of strong interactions. Comparison of structure functions measured in different processed (νN, eN, μN, Drell-Yan) is an important test of our understanding of the "hard scattering" processes. Using measured structure functions together with fragmentation functions we can learn more about quark-quark forces from data on large p_T processes in hadron-hadron collisions.

Neutrinos as a tool of probing nucleons have some unique features:

i) Owing to the V - A structure of weak interactions they allow the separate study of the quark and antiquark content of the nucleon. This means that at the same time we may study the valence quark distribution, for which some theoretical predictions are particularly simple.

ii) They allow independent studies of separate flavours, either by choosing the beam (ν,$\bar\nu$) or some specific final state, for example, $\bar\nu$N $\rightarrow \mu^+\mu^-$ probes the predominantly strange antiquark distribution

$$\frac{d\sigma^{\bar\nu N \rightarrow \mu^+\mu^-}}{dxdy} \approx \frac{G^2ME_\nu}{\pi}\left\{2\bar{s}(x)\ \cos^2\ \theta_c + \left[\bar{u}(x) + \bar{d}(x)\right]\ \sin^2\ \theta_c\right\}.$$

$$(8)$$

Experiments

Experiments which have contributed to our knowledge of nucleon structure functions are either those being done with big bubble chambers (usually filled with heavy liquid) or with large calorimeters (see Table 1). The resolution of different experiments is shown in Fig. 5. The resolution of BEBC is typical of all bubble chamber experiments. From Fig. 5 one can see that muon momentum is measured better in bubble chambers (the same is true for the muon angle), whereas counter experiments measure more precisely the hadron energy. Muon identification is also better in the case of counter experiments.
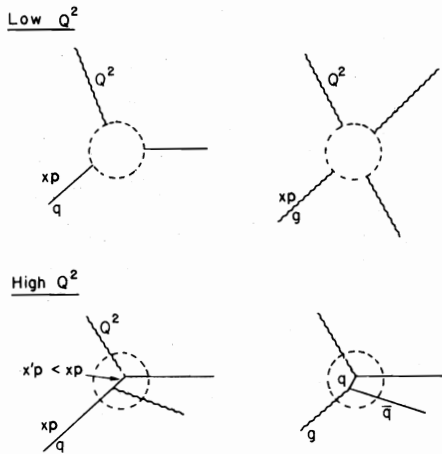

Fig. 3 The basic processes contributing to the Q^2 evolution of the structure functions.

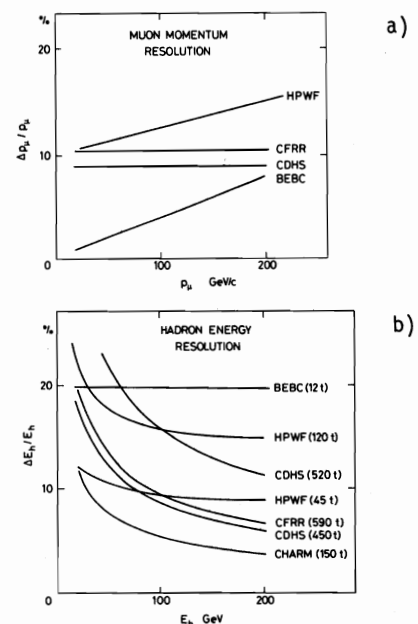Fig. 4 The expected change of the structure functions with Q^2.

Fig. 5 Resolution of different experiments measuring the nucleon structure functions: a) hadron energy resolution; b) muon momentum resolution.

Table 1

List of experiments

Collaboration	Target	E_ν	No. of events $\bar\nu$	No. of events ν	Measured quantities
ABCLOS (Gargamelle)	propane/freon	2 – 10	2 000	3 000	$F(x,Q^2)$, R, $\bar q(x)$
ABCLOS (BEBC)	H_2/N_e	20 – 200	270	1 270	$F(x,Q^2)$, R, $\bar q(x)$
CITFR	Fe	45 – 205	12 000	18 000	R
CDHS	Fe	30 – 200	6 200	23 000	$F(x,Q^2)$, R, $\bar q(x)$
HPWFRO	H-C-Fe	20 – 200	5 180	4 900	$F(x)$, R, $\bar q(x)$
ACMP	H_2	$\sim$ 30	2 275		$u(x)$, $\bar d(x)$
FIIM	H_2/N_e	20 – 50	2 500		R
CDHS	Fe	20 – 200	12 000	60 000	$\bar s(x)$
ABCLOS (BEBC)	H_2/N_e	20 – 200	650	1 700	$F(x,Q^2)$
CHARM	Fe	$\sim$ 30	3 400		$P(\mu^+)$

ABCLOS = Aachen-Bonn-CERN-London-Oxford-Saclay
CITFR = Cal. Tech.-Fermilab-Rockefeller
CDHS   = CERN-Dortmund-Heidelberg-Saclay
HPWFRO = Harvard-Pennsylvania-Wisconsin-Fermilab.-Rutgers-Ohio
ACMP   = Argonne-Carnegie-Melon-Purdue
FIIM   = Fermilab.-ITEP-IHEP-Michigan
CHARM = CERN-Hamburg-Amsterdam-Rome-Moscow

V - A Structure of Weak Charged Current

As mentioned before, the expression for the cross-section in terms of structure functions was derived under the assumption of a V-A interaction. From low-energy experiments (mainly decay studies) we know that weak current is of the V-A type, and we assume therefore that the same is true at energies as high as 200 GeV. Studies of y distribution do not contradict this assumption [i.e. $d\sigma/dy \sim a + b(1-y)^2$], but there is a so-called "confusion" theorem which states that for any mixture of V and A coupling there is a mixture of S, P, T coupling yielding the same cross-section.

What makes V and A coupling different from the others is the helicity of the final lepton. V and A preserve helicity of the lepton, whereas S, P, or T flip it. For example, μ^+ emerging from an antineutrino interaction will have a polarization of +1 if the interaction proceeds via vector or axial current, or it will have a polarization of -1 if the current is S, P, or T.

Measurement of the polarization of μ^+ was done by the CHARM Collaboration[1] using the CDHS detector as a target (see Fig. 6). Muons stopped in the CHARM apparatus and precessed in the magnetic field there. Forward-backward asymmetry of emitted electrons as a func-
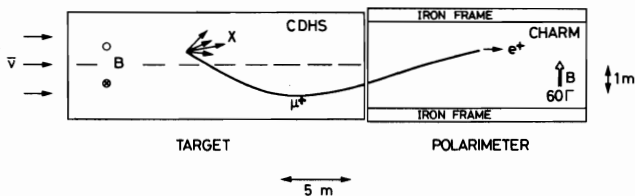
tion of time provides information on μ polarization (Fig. 7). Having 3400 stopping μ^+ with

$$\langle p_\mu \rangle = 16 \text{ GeV}$$

$$\langle E_\nu \rangle = 27 \text{ GeV}$$

$$\langle Q^2 \rangle = 3 \text{ GeV}^2 \ ,$$

they find $(B-F)/(B+F) = (0.14 \pm 0.02) \cos(\omega t - \pi \pm 0.2)$ + const., which can be translated into the muon polarization $P(\mu^+) = 1.09 \pm 0.22$. On this basis they can set a limit on the contribution of other than V and A couplings to the total cross-section

$$\frac{\sigma^{S,P,T}}{\sigma_{tot}} < 0.18 \ (95\% \text{ C.L.}) \ .$$

Fig. 6 The experimental set-up used for the measurement of the muon polarization.
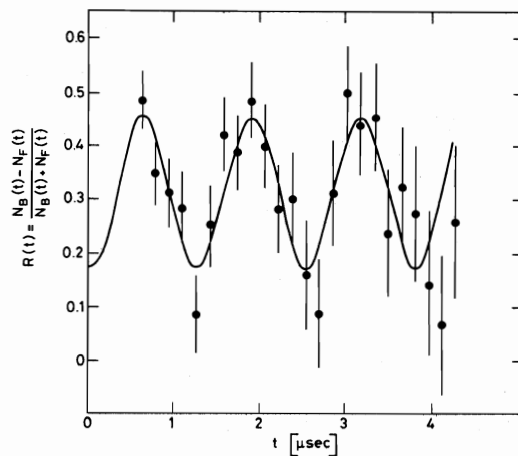

Fig. 7 Forward-backward asymmetry of emitted electrons as a function of time.

Shape of Structure Functions

To have an idea of what structure functions look like, let us first look at the structure functions as a function of x only (i.e. averaged over all E_ν or Q^2). One usually assumes the Callan-Gross relation (5) to reduce the number of functions to be determined to two. Structure functions can be determined in two ways:

i) by fitting the population of the x-y plane with formula (3); this technique was used by the ACMP collaboration[2];

ii) in the case of an isoscalar target and having both ν and $\bar\nu$ data one can form the appropriate combinations

$$\frac{d^2\sigma^\nu}{dxdy} + \frac{d^2\sigma^{\bar\nu}}{dxdy} = \frac{G^2 M E_\nu}{\pi} F_2(x)\left[1 + (1-y)^2\right]$$

$$\frac{d^2\sigma^\nu}{dxdy} - \frac{d^2\sigma^{\bar\nu}}{dxdy} = \frac{G^2 M E_\nu}{\pi} xF_3(x)\left[1 - (1-y)^2\right].$$

(9)

These formulae are subject to small corrections due to differences between the strange and charmed sea. This method was applied by the ABCLOS[3], CDHS[4], and HPWFRO[5] groups. Figure 8 shows $F_2(x)$ as measured by the different groups. CDHS, ABCLOS, and HPWFRO results for an I = 0 target roughly agree with each other (the slight discrepancy, especially at large x, is probably due to some experimental problems of HPWFRO[5]), whereas $F_2^\nu p(x)$ of ACMP is definitely higher. This difference is interpreted to be due to the fact that the incoming ν or $\bar\nu$ sees $1\frac{1}{2}$ valence quarks in the "isoscalar" nucleon, but the $\bar\nu$ sees two valence quarks in p. After correction for this effect (see Fig. 9), $F_2^{\bar\nu}p$ still seems to be slightly wider than $F_2(x)$ for the isoscalar target, which may indicate some difference between u and d quark distributions.

In Fig. 10 $xF_3(x)$ from CDHS and HPWFRO is plotted. The agreement is reasonable, although at small x there is some discrepancy. The small x region is crucial for testing the Gross-Llewellyn-Smith sum rule, so understanding of this discrepancy is very important.
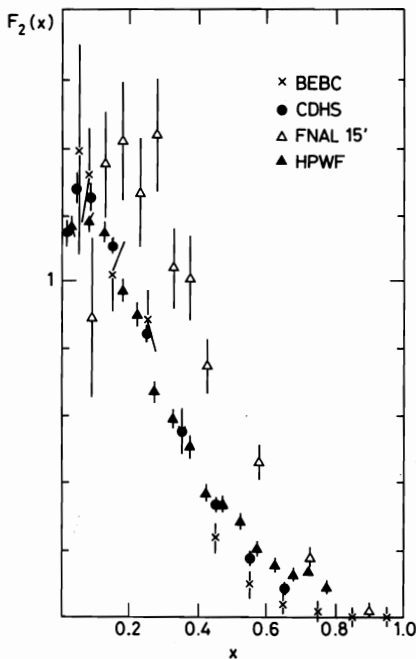

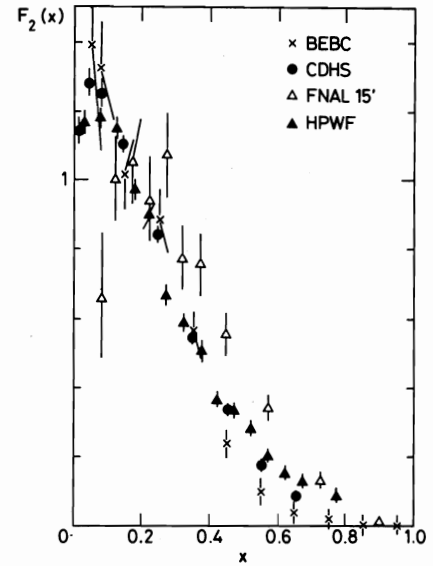Fig. 8 The structure function $F_2(x)$ from different experiments.

Fig. 9 The $F_2(x)$ from different experiments. The ACMP (15') results have been scaled down by a factor of $\frac{3}{4}$.
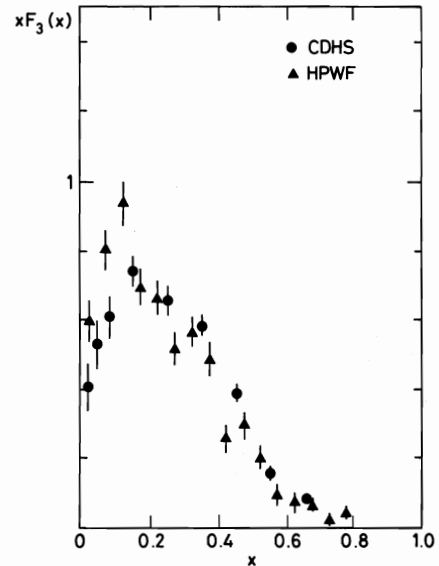

Fig. 10 $xF_3(x)$ as measured by CDHS and HPWFRO.

Antiquarks and Sea Composition

The sea of $q\bar q$ is responsible for the difference between $F_2(x)$ and $xF_3(x)$. We can determine the amount and distribution of the antiquarks in the following ways:

i) Fitting y-distributions with

$$\frac{d\sigma^{\nu N}}{dxdy} = \frac{G^2 M E_\nu}{\pi}\left[q^\nu(x) + \bar q^\nu(x)(1-y)^2\right]$$

$$\frac{d\sigma^{\bar\nu N}}{dxdy} = \frac{G^2 M E_\nu}{\pi}\left[\bar q^{\bar\nu}(x) + q^{\bar\nu}(x)(1-y)^2\right]$$

(10)

or with formulae integrated over x.

ii) Comparing ν- and $\bar\nu$-distributions at $y \approx 1$. From Eqs. (10) one derives

$$\frac{(d\sigma^{\bar\nu N}/dx) - (1-y)^2\,(d\sigma^{\nu N}/dx)}{\sigma^\nu + \sigma^{\bar\nu}}\Bigg|_{y\approx 1} =$$

$$= \frac{\bar q^\nu(x)}{\int[q(x) + \bar q(x)]\,dx} = \frac{\bar q^\nu(x)}{Q + \bar Q} = \frac{\bar q(x) + s(x)}{Q + \bar Q}\ . \quad (11)$$

iii) From dilepton events ($\mu^+\mu^-$ in particular)

$$\sigma^{\nu N \to \mu^+\mu^-} = \frac{G^2 M E_\nu}{\pi}\left[(U+D)\,\sin^2\theta_c + 2S\,\cos^2\theta_c\right]BR(c \to \mu^+)$$

$$\qquad\qquad\qquad\qquad\qquad\qquad\qquad\qquad (12)$$

$$\sigma^{\bar\nu N \to \mu^+\mu^-} = \frac{G^2 M E_\nu}{\pi}\left[(\bar U+\bar D)\,\sin^2\theta_c + 2\bar S\,\cos^2\theta_c\right]BR(\bar c \to \mu^-).$$

where $BR(c \to \mu^\pm)$ is the branching ratio for the c quark decay into a muon. From this one gets

$$\frac{2\bar S}{\bar U + \bar D} = \tan^2\theta_c\ \frac{1}{\dfrac{\sigma(\nu N \to \mu^+\mu^-)}{\sigma(\bar\nu N \to \mu^+\mu^-)} - 1}\ .$$

In Table 2 we summarize results on the total amount of antiquarks. All groups agree that at high energies antiquarks carry $\sim 15\%$ of the total quark momentum; at very low energies this drops to $\sim 7\%$.

Table 2

Momentum fraction carried by antiquarks

Collaboration	E_ν	$\dfrac{\bar Q + \bar S}{Q + \bar Q}$
ABCLMOP[6]	> 1	0.07 ± 0.04
FIIM[7]	10-200	0.14 ± 0.03
HPWFRO[8]	< 45	0.11 ± 0.02
	> 80	0.17 ± 0.02
ABCLOS[3]	$Q^2 > 3$	0.11 ± 0.03
CDHS[4]	30-200	0.16 ± 0.01
FIIM[9]	20-50	0.13 ± 0.02
ABBLS[10]	10-100	0.05 ± 0.05
ACMP[2]	~ 30	0.16 ± 0.06

ABCLMOP = Aachen-Brussels-CERN-London-Milan-Orsay-Palaiseau·

ABBLS = Aachen-Bergen-Brussels-London-Strasbourg.

As the information on antiquarks is coming predominantly from antineutrinos, the measured quantity is not $\bar Q/(Q+\bar Q)$ but rather $(\bar U + \bar D + 2\bar S)/(Q+\bar Q) = (\bar Q + \bar S)/(Q+\bar Q)$.

The $\bar\nu p$ experiment measures $2(\bar D + \bar S)/(Q + \bar Q)$. The x-distribution of antiquarks is shown in Fig. 11. Data show that the $q\bar q$ sea is concentrated at small x and there is practically no sea above x = 0.4 (the large x tail in the case of the HPWFRO data is probably an experimental artifact[5]).
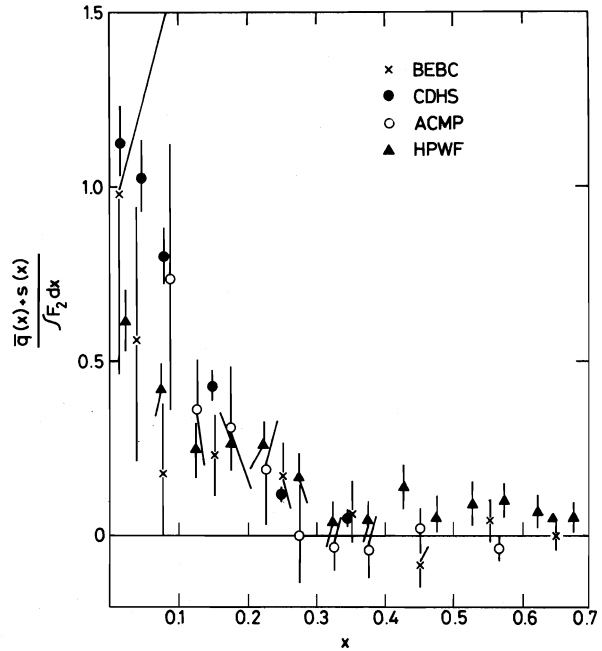

Fig. 11 The x distribution of antiquarks.

If one parametrizes the sea distribution as $(1-x)^n$ then the value of n is given in Table 3.

Table 3

Power of (1 - x) for sea distribution

Collaboration	n	Method
ABCLOS	$4.9\ ^{+\ 2.4}_{-\ 1.7}$ [3]	$\bar\nu - \nu$
CDHS	6.5 ± 0.5 [4]	$\bar\nu - \nu$
HPWFRO	4.6 ± 0.8 [5]	$\bar\nu - \nu$
	9.5 ± 2 [8]	$\dfrac{d\sigma^{\bar\nu N}}{dy}$
ACMP	10.3 ± 3.4 [2]	$\dfrac{d\sigma^{\bar\nu p}}{dy}$

One should notice that independent measurements of the sea x-distribution by massive muon pair production in hadron-hadron experiments (Drell-Yan) give very similar results[11] (see Fig. 12). There is however some discrepancy in the normalization; Drell-Yan data are a factor ~ 2 higher than neutrino data. This could be due to some higher order QCD corrections for a Drell-Yan mechanism[12] or to some experimental problems[13].
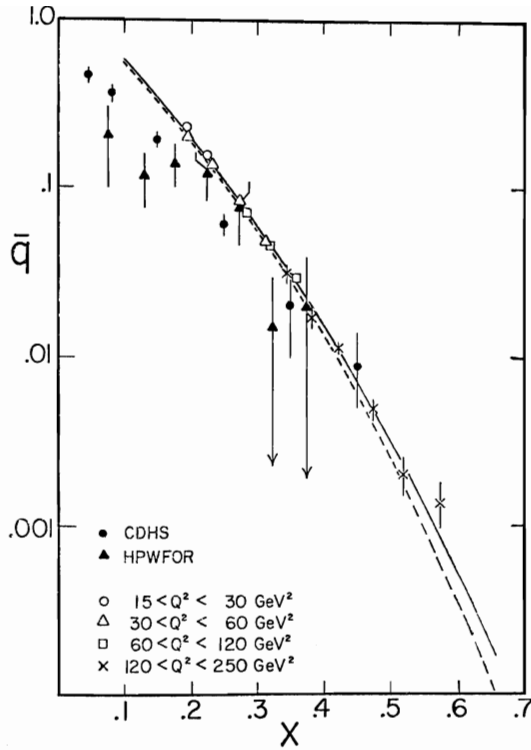
Fig. 12 Comparison of x-distribution measured in neutrino interactions with the Columbia-Fermilab-Stony Brook results from the massive $\mu^+\mu^-$ pair production (open symbols).

From opposite sign dimuons we learn that the sea is not SU(3) symmetric, i.e. strange antiquarks carry less momentum than $\bar{u}$ or $\bar{d}$ (see Table 4).

Table 4

Fraction of momentum carried by strange quarks

Collaboration	E_μ	$2\bar{S}/(Q + \bar{Q})$
CDHS	< 200	0.05 ± 0.02 [4]
HPWFRO	> 80	0.07 ± 0.06 [14]
CDHS	< 200	0.03 ± 0.01 [15]

HPWFRO data suggest $\bar{S}/\bar{U} = 0.5$, whereas from the CDHS results we get $\bar{S}/\bar{U} \approx \frac{1}{4}$. The fit to the x-distribution yields $s(x) \sim (1-x)$ to the power of $10^{+1.3}_{-1.4}$, suggesting that strange quarks have a somewhat steeper distribution than light quarks.

Callan-Gross Relation

The naïve quark-parton model prediction $2xF_2(x) = F_2(x)$ (Callan-Gross) is not valid if partons have some intrinsic transverse momentum. In this case one expects[16] $R = 4\langle p_T^2\rangle/Q^2$, where $R = \sigma_S/\sigma_T = [F_2(1 + Q^2/\nu^2) - 2xF_1]/2xF_1$. Violation of the Callan-Gross relation is predicted by QCD as well. From the very fact that y-distributions for ν and/or $\bar{\nu}$ are consistent with the $a + b(1-y)^2$ form we know that the Callan-Gross relation is certainly a good approximation.

To look for violation of the Callan-Gross relation one defines

$$R' = \frac{F_2 - 2xF_2}{F_2} \qquad \left(R' < R = \frac{\sigma_S}{\sigma_T}\right).$$

R' can be evaluated in different ways:

i) by looking for the $(1-y)$ term in ν or $\bar{\nu}$ y-distribution;

ii) by fitting the sum of ν and $\bar{\nu}$ y-distributions with

$$\frac{d\sigma^\nu}{dy} + \frac{d\sigma^{\bar{\nu}}}{dy} = \frac{G^2 ME_\nu}{\pi} F_2[1 + (1-y)^2 - y^2 R']$$

(see Fig. 13).

To avoid uncertainties due to possible scaling violations one should perform this fit keeping x and Q^2 constant (Fig. 14) or $\nu = yE_\nu$ constant (Fig. 15).
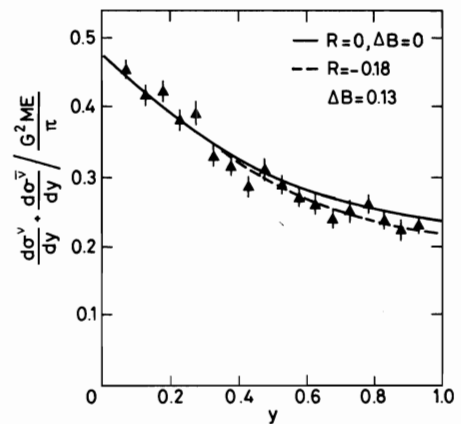

Fig. 13 Fit to the $\nu + \bar{\nu}$ y distribution with and without the Callan-Gross violating term (HPWFRO).
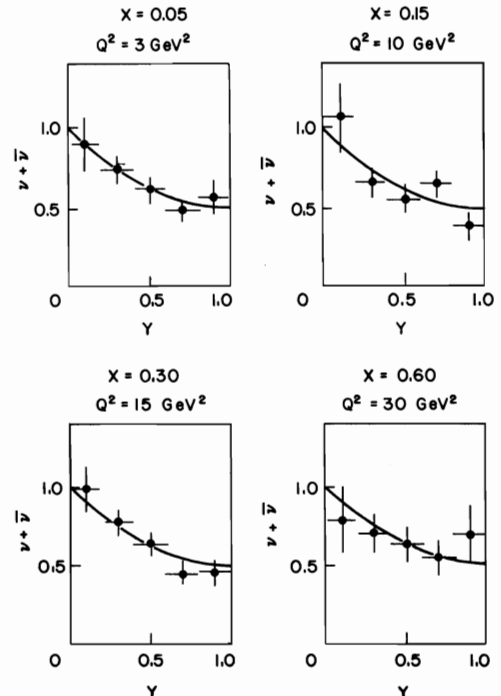

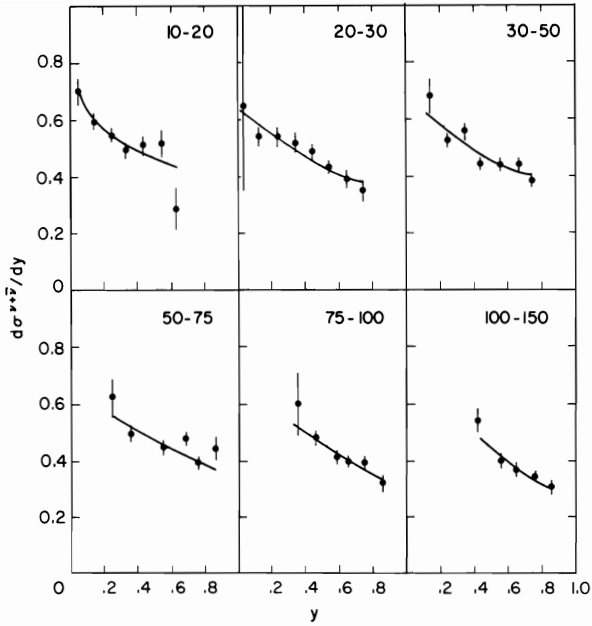Fig. 14 Fits to the y distributions for different x and Q^2 bins (ABCLOS).

Fig. 15 Fits to the y distributions for different ν bins (CDHS).

$$\frac{\sigma^{\nu n}}{\sigma^{\nu p}} = \frac{\int [u(x) + s(x) + \frac{1}{3}\,\bar{d}(x)]dx}{\int [d(x) + s(x) + \frac{1}{3}\,\bar{u}(x)]dx} \approx 1.9$$

$$\frac{\sigma^{\bar{\nu} n}}{\sigma^{\bar{\nu} p}} = \frac{\int [\frac{1}{3}\,d(x) + \bar{d}(x) + \bar{s}(x)]dx}{\int [\frac{1}{3}\,u(x) + \bar{d}(x) + \bar{s}(x)]dx} \approx 0.55 \ .$$

(13)

Nature offers no neutron target; $\sigma^{\nu n}$ has to be extracted from deuterium, neon, or other heavy liquid data. Experimental results are in good agreement with predictions (see Table 6), although they are not precise enough to distinguish naïve from more sophisticated models. The Stony Brook-Tohoku-Chicago-Maryland-Tufts (SBTCMT) Collaboration[20] has shown that the x-distribution from νn is broader than that from νp (see Fig. 16), which suggests that fast quarks in protons are likely to be u quarks [in agreement with SLAC results on $(\sigma^{ep}/\sigma^{en})(x)$].

Table 6

Ratio of neutron and proton cross-sections

Group	E_ν	$\sigma^{\nu n}/\sigma^{\nu p}$
ANL	1.5 - 6	1.95 ± 0.21 [21]
BNL	< 10	1.48 ± 0.17 [22]
ABCOPP	1 - 10	2.08 ± 0.15 [23]
BBBLPRS	∿ 30	1.97 ± 0.38 [24]
SBTCMT	∿ 30	1.74 ± 0.25 [20]
Group	E_ν	$\sigma^{\bar{\nu} n}/\sigma^{\bar{\nu} p}$
BBMST	< 5	0.46 ± 0.1 [25]
FIIM	∿ 30	0.51 ± 0.1 [26]

ABCOPP = Aachen-Brussels-CERN-Orsay-Padova-Palaiseau
BBBLPRS = Bari-Birmingham-Brussels-London-Palaiseau-Rutherford-Saclay
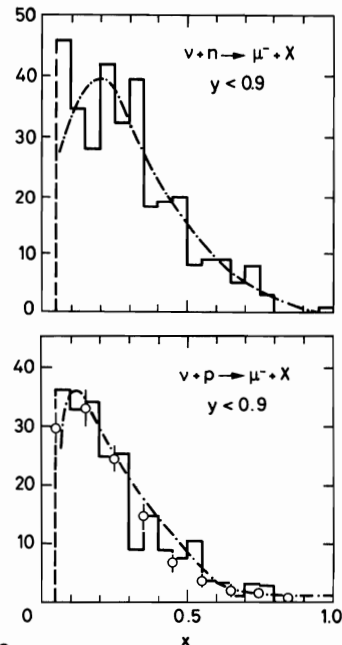BBSMT = Bari-Bergen-Milan-Strasbourg-Torino

This is generally not done. From Table 5 one sees that neutrino data are not yet very conclusive. Differences

Table 5

Callan-Gross Violation, R′

Group	R′	Comments
CITFR	0.17 ± 0.09 [17]	
ABCLOS	0.32 ± 0.15 [3]	$Q^2 < 1$
ABCLOS	0.11 ± 0.14 [3]	
CDHS	-0.03 ± 0.05 [4]	
HPWFRO	0.18 ± 0.07 [5]	Radiative corrections applied
CDHS	0.03 ± 0.05(±0.1) [19]	" "
FIIM	-0.12 ± 0.16 [7]	

between different experiments are much larger than the effect itself. One should remember that besides other systematic problems, the Callan-Gross relation is very sensitive to radiative corrections. Unfortunately there are two different recipes for doing these corrections which do not agree with each other. Uncertainty in radiative corrections produces uncertainty in R′ of the order of 0.05-0.07, i.e. comparable with R′ itself.

There is clearly much more work to be done, both theoretically and experimentally, before we can reach some conclusion on R′ and its possible dependence on Q^2 or x.

Proton-neutron comparison

If there would be no sea inside the nucleon the quark-parton model would predict $\sigma^{\nu n}/\sigma^{\nu p} = 2$, whereas $\sigma^{\bar{\nu} n}/\sigma^{\bar{\nu} p} = \frac{1}{2}$. The presence of the $q\bar{q}$ sea, or the difference in the u and d quarks x-distributions modify slightly this prediction:

Fig. 16 Comparison of the x-distributions for neutrino-proton and neutrino-neutron interactions.

Other Tests of the Quark-Parton Model

The Gross-Llewellyn-Smith sum rule allows us to count valence quarks in the target. The results of these tests are in good agreement with expectations

$$\int_0^1 \frac{xF_3(x)}{x}\,dx = \begin{cases} 3.0 \pm 0.6 & \text{ABCLMOP } [18] \\ 3.2 \pm 0.5 & \text{CDHS} \quad [4] \\ 2.8 \pm 0.5 & \text{ABCLOS} \quad [3] \\ 2.8 \pm 0.2 & \text{HPWFRO } [5] \end{cases}$$

According to our present understanding, the structure functions seen by charged current (CC) ($W^\pm$) or neutral current (NC) (Z^0) should be very similar. For the moment we do not have measurements of the structure functions in NC interactions but comparison of x-distributions for CC and NC events shows that they are similar[27] (see Fig. 17). In the same way one expects that electron neutrinos see the same structure of the
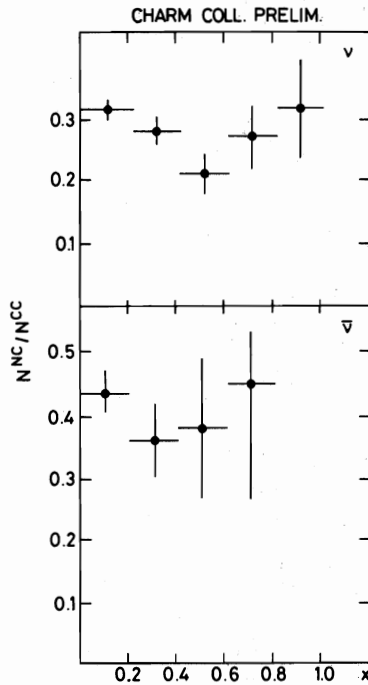
CHARM COLL. PRELIM.

Fig. 17 Ratio of the x-distributions for the neutral and charged current interactions (CHARM).

nucleon as ν_μ; data are very poor for the moment however. General characteristics of ν_e induced interactions are roughly the same as those for ν_μ, showing that there is no dramatic difference between both classes of interactions[28].

To summarize this section let us note that the so-called naïve quark-parton model is in surprisingly good agreement with the high energy neutrino data, both qualitatively and quantitatively.

Scale-Breaking Effects

Scaling assumption says that structure functions depend on two variables ν and Q^2 only through their ratio, $x = Q^2/2M\nu$. Some deviations are expected, however, causing Q^2 (or ν) dependence of structure functions. To see if such effects are present in the data we compare in Fig. 18 the shape of $F_2(x)$ as measured at different energies[4,29,30] (corresponding to different average Q^2). Scaling is obviously broken, so we should study structure functions as functions of two variables: Q^2 and ν, or x and Q^2, or x and ν. Theoreticians like
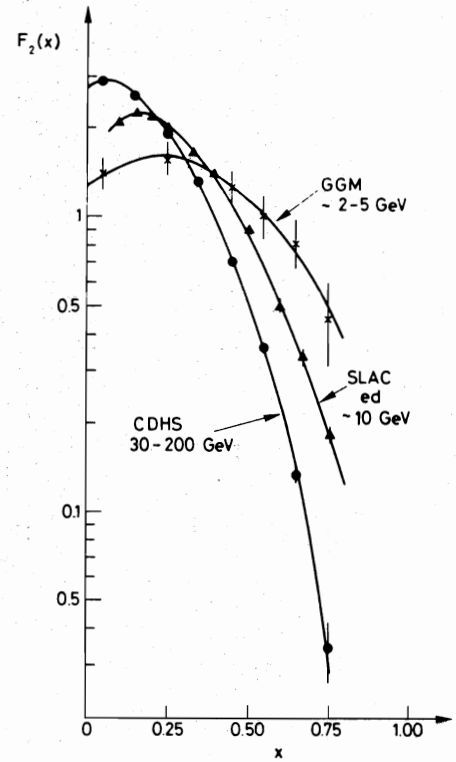
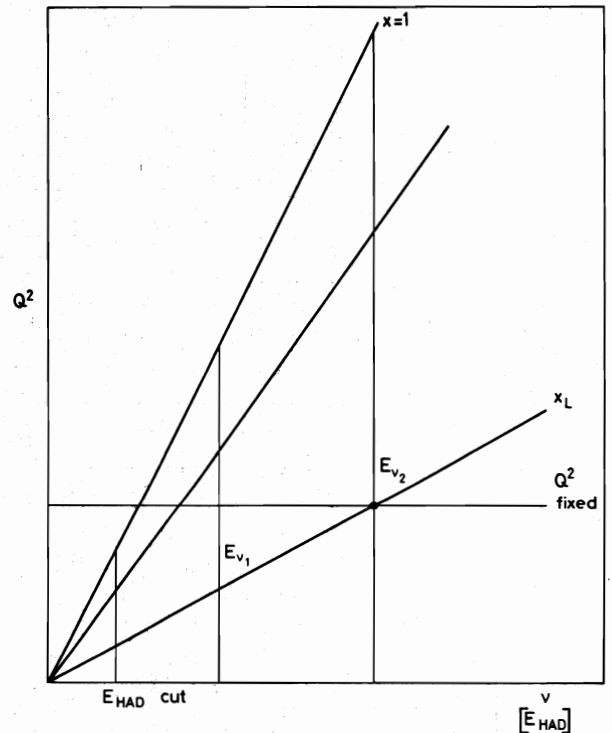Fig. 18 Comparison of the $F_2(x)$ structure function seen in different lepton energy domains.

Fig. 19 The $Q^2 - \nu$ plot.

x and Q^2 very much, as all predictions are easy to compute at fixed Q^2. From the experimental point of view this is a bad choice. From Fig. 19 we see that at fixed Q^2 there is always some low-x region which will not be accessible, even at extremely high energies. Counter experiments, which provide high-statistics data, do not measure low hadron energies accurately enough; this makes the large-x region unavailable at low Q^2. At fixed ν the whole x range can be studied.
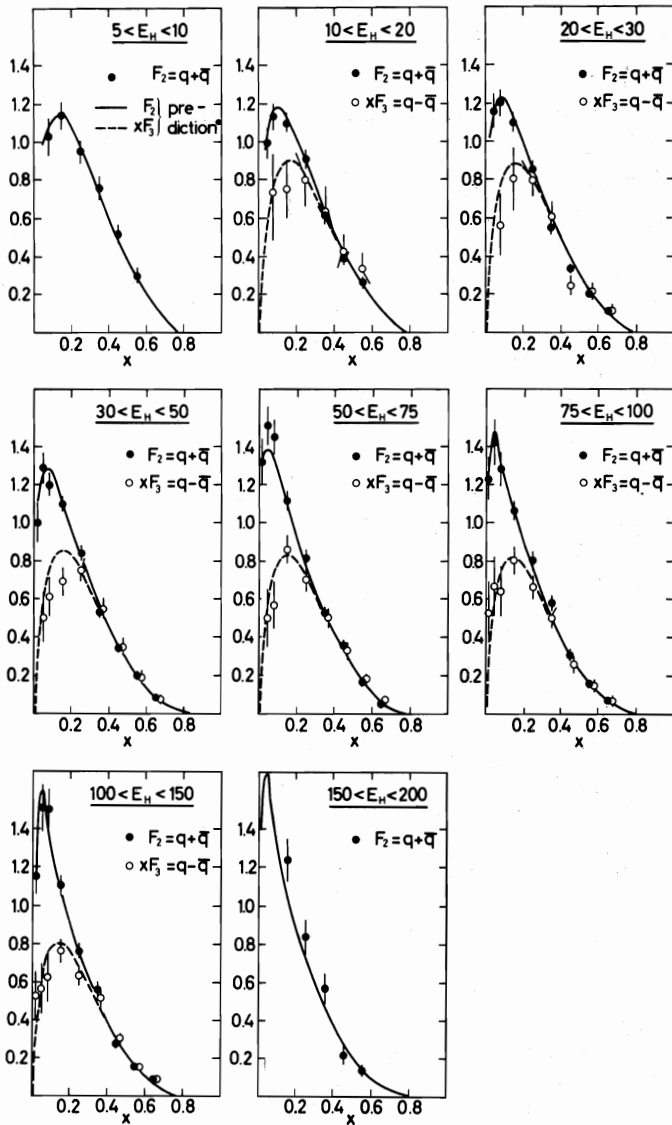
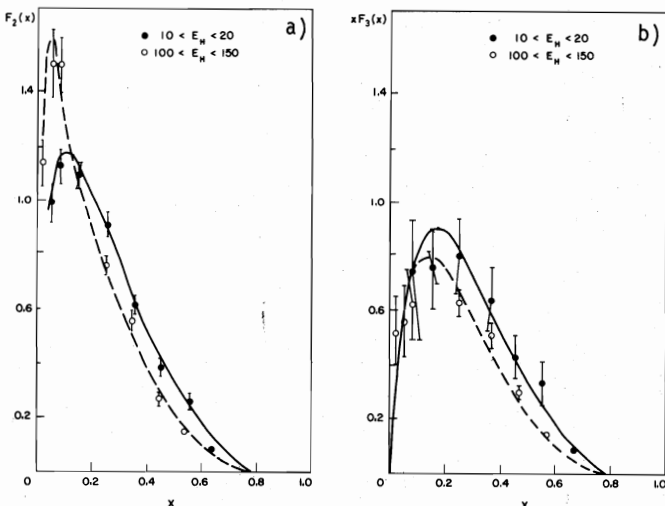Fig. 20 $F_2(x)$ and $xF_3(x)$ for different ranges of the hadron energy (CDHS).

Fig. 21 Comparison of a) $F_2(x)$, b) $xF_3(x)$, at low and high hadron energy.

From CDHS results[4] (Fig. 20) one sees clearly that structure functions shrink as ν increases; in case of $F_2(x)$ one sees in addition a substantial rise at small x. This is seen more clearly in Fig. 21, where we compare two extreme ν bins. In Fig. 22 we present the same data together with the ABCLOS results in the usual way, i.e. F_2 and xF_3 at fixed x versus Q^2. Qualitative agreement with QCD predictions is obvious; what about quantitative tests?

QCD Predictions for Q^2 Evolution of Structure Functions

In general Q^2 evolution of quark distribution depends on the initial distribution of both quarks and gluons. Predictions for non-singlet (NS) structure functions [for example $xF_3(x)$, $u(x) - d(x)$ ...] do not depend on gluon distribution, so they are more reliable.

In the first order in α_s Q^2 evolution of structure functions is governed by the Altarelli-Parisi[31] equations. Their solutions are particularly simple for the moments of the structure functions

$$M_N(Q^2) = \int\limits_0^1 x^{N-2} F(x,Q^2)\, dx \ . \tag{14}$$

For non-singlet functions we have

$$M_N^{NS}(Q^2) = M_N^{NS}(Q_0^2) \left[\frac{\log\ (Q^2/\Lambda^2)}{\log\ (Q_0^2/\Lambda^2)} \right]^{-d_N} \tag{15}$$

and for singlet functions

$$M_N^S(Q^2) = \left[(1 - \alpha_N) M_N^S(Q_0^2) - \beta_N M_N^G(Q_0^2) \right] \left[\frac{\log\ (Q^2/\Lambda^2)}{\log\ (Q_0^2/\Lambda^2)} \right]^{-d_N^+} +$$

$$+ \left[\alpha_N M_N^S(Q_0^2) + \beta_N M_N^G(Q_0^2) \right] \left[\frac{\log\ (Q^2/\Lambda^2)}{\log\ (Q_0^2/\Lambda^2)} \right]^{-d_N^-} , \tag{16}$$

where α_N, β_N, d_N, $d_N^\pm$ are numbers given by QCD, whereas $M_N^{NS}(Q_0^2)$, $M_N^S(Q_0^2)$, $M_N^G(Q_0^2)$ are the moments of non-singlet and singlet functions and gluons, respectively at some Q_0^2.

From Eq. (15) another prediction can be derived, which is independent of Λ

$$\log M_N^{NS}(Q^2) = \frac{d_N}{d_{N'}}\ \log M_{N'}^{NS}\ (Q^2) + const. \tag{17}$$

Comparison of the experimental data with the predictions listed above may serve several purposes:

i) We can check if there is such a value of Λ that Eqs. (15) and (16) describe Q^2-dependence of measured structure functions. At the same time, we determine the value of Λ as well as some parameters of the gluon distribution [in case of the analysis of $F_2(x,Q^2)$ data].

ii) Comparing Eq. (17) with the data we can check the values of d_N predicted by QCD. This test is sensitive to the assumed spin of gluons.
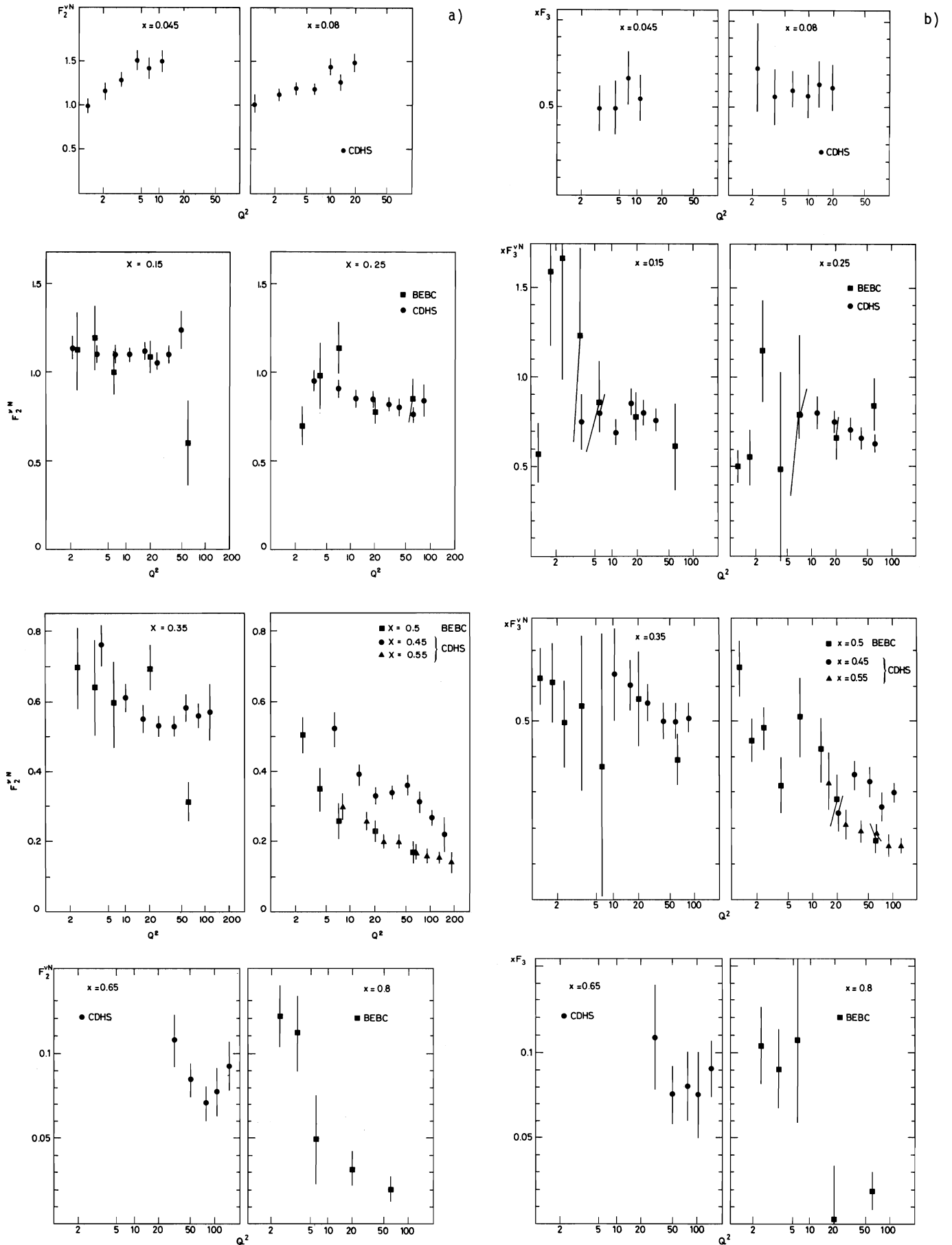
Fig. 22 a) $F_2(x)$ in different x bins as a function of Q^2. b) $xF_3(x)$ in different x bins as a function of Q^2.

Experimental Tests of QCD Predictions

QCD predictions for the evolution of structure functions are in the form of differential equations, whereas those for evolution of moments have the form of simple analytical formulae. On the other hand, moments have their disadvantages: some theoretical problems are discussed by Ellis[32]; let us mention here one experimental problem. To calculate moments one has to perform integration over x from 0 to 1 at fixed Q^2. Apart from resolution problems at large x (especially for counter experiments) the low-x region is not accessible kinematically -- one has to extrapolate data to x = 0 and x = 1.

To account for target mass effects (i.e. the fact that our actual Q^2 is not much bigger than 1 GeV) one has to use so-called Nachtmann moments[33]. This is important whenever low-Q^2 data (i.e. below $\approx$ 10 GeV^2) are used. Before we go to the moments analysis let us see what we can learn from structure functions themselves.

Buras-Gaemers Fit

i) xF₃ case

Buras and Gaemers[34] have shown that if $xF_3(x,Q^2)$ could be parametrized by

$$xF_3(x,Q_0^2) = \frac{3}{B(\eta_1,\eta_2+1)} x^{\eta_1(s)}(1-x)^{\eta_2(s)} \qquad (18)$$

where

$$s = \frac{\log\ (Q^2/\Lambda^2)}{\log\ (Q_0^2/\Lambda^2)} \quad \text{and} \quad B \text{ is the Euler } \beta\text{-function,}$$

then the QCD moments equations will be fulfilled, provided

$$\eta_1(s) = \eta_{10} + 4/25\ \eta_{11}s, \quad \eta_2(s) = \eta_{20} + 4/25\ \eta_{22}s\ .$$

The CDHS Collaboration[35] has shown that this parametrization provides a good description of their data (see Fig. 23) yielding at $Q_0^2 = 20$

$$\Lambda = 0.55 \pm 0.15(\pm 0.1)\ \text{GeV}$$
$$\eta_1 = 0.51 \pm 0.02 - 4/25 \times 0.83\ s$$
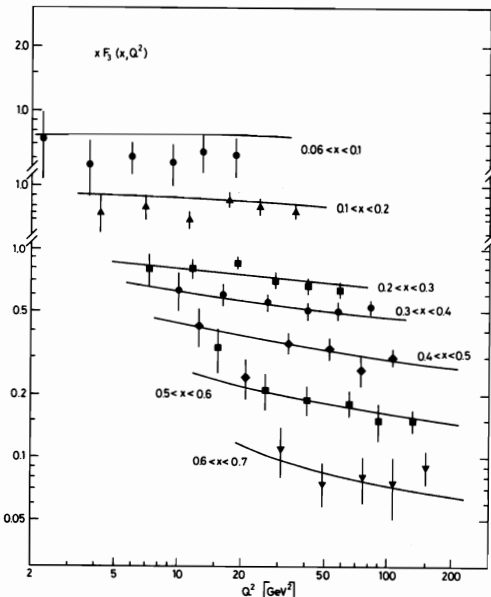$$\eta_2 = 3.03 \pm 0.09 + 4/25 \times 5.0\ s\ .$$

Fig. 23 Comparison of the Buras-Gaemers fit with the xF₃(x) data of CDHS.

ii) F₂ case

If we parameterize the sea as $A(s)(1-x)^{P(s)}$, then

$$F_2(x,Q^2) = xF_3(x,Q^2) + A(s)(1-x)^{P(s)} \qquad (19)$$

where $xF_3(x,Q^2)$ is given by Eq. (18). This form does not satisfy the QCD moments equation (16) exactly but is a very good approximation of the exact solution in the Q^2 range where we are[36]. To fit data with formula (19) one needs one more free parameter, i.e. the third moment of gluon distribution (the second moment is given by momentum conservation). CDHS data[35] yield

$$\Lambda = 0.47 \pm 0.11(\pm 0.1)$$
$$\eta_1 = 0.56 \pm 0.02 - 4/25 \times 0.92\ s$$
$$\eta_2 = 2.71 \pm 0.11 + 4/25 \times 5.08\ s$$
$$A(Q_0^2 = 5\ \text{GeV}) = 0.99 \pm 0.07$$
$$P(Q_0^2 = 5\ \text{GeV}) = 8.1 \pm 0.7$$
$$M_3^G(Q_0^2 = 5\ \text{GeV}) = 0.105 \pm 0.02\ .$$

The agreement of the data with this parametrization is again satisfactory (see Fig. 24). In addition one sees that F_2^{ed} of SLAC (not used in this fit) multiplied by 18/5 agrees very well with fitted curves. This fact allows the CDHS group to calculate moments of structure functions using SLAC data at high x. Repeating these fits using different Q_0^2 they were able to study the Q^2 evolution of the nucleon structure (see Fig. 25). As

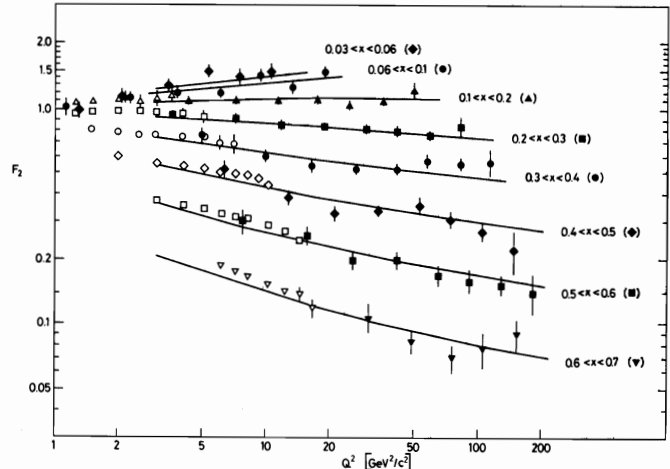Fig. 24 Comparison of the Buras-Gaemers fit with the F₂(x) data of CDHS. The open symbols represent SLAC electron-deuteron data.
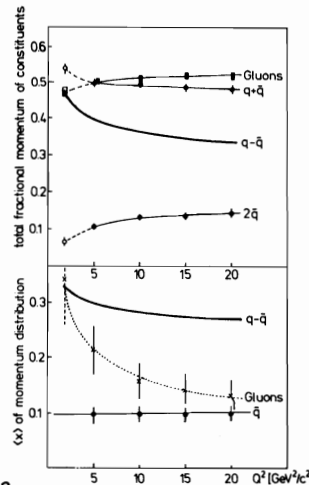
Fig. 25 The total fractional momentum and average of x of different kinds of constituents as a function of Q^2.

we see, although momentum-sharing between quarks and gluons almost does not change, gluon distribution shrinks very fast and valence quark distribution shrinks slowly, whereas the shape of the sea distribution remains unchanged up to Q^2 = 20 GeV.

Gluon Distribution

Baulieu and Kounnas[37] have pointed out that if one measures the derivatives $\partial F_2(x,Q^2)/\partial \ln Q^2$, then it is possible to invert the Altarelli-Parisi equations to obtain gluon distribution $G(x,Q^2)$. Following their recipe CDHS[19] obtains $G(x,Q^2 = 20$ GeV$) \sim (1-x)^{5.6}$ (see Fig. 26).
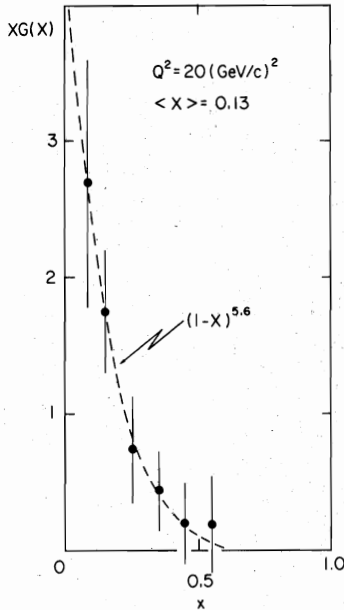
Fig. 26 The x-distribution of gluons, at Q^2 = 20 GeV^2.

Moments Analysis

QCD predicts that the log of one xF_3 moment plotted against the log of another xF_3 moment should give a straight line with a slope, which depends on the spin of the gluon. Data of ABCLOS[3] and CDHS[38] are very well consistent with this prediction (see Fig. 27). The results of corresponding fits are compared with QCD (vector gluons) or QCD-like theory with scalar gluons
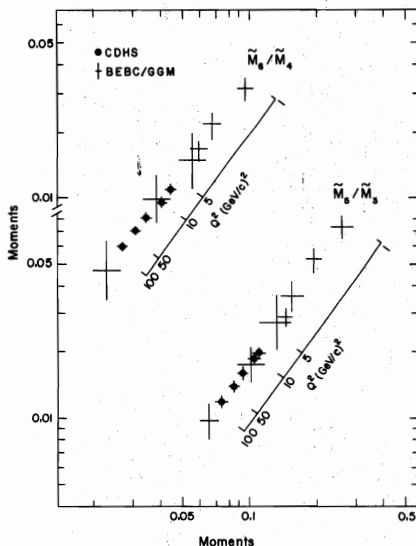
Fig. 27 The dependence of the log of one moment on the log of another moment.

Table 7

Ratio of anomalous dimensions from xF_3 moments

	ABCLOS	CDHS		Theory	
$d_i d_j$	Nachtmann	Ordinary	Nachtmann	Vector	Scalar
d_5/d_3	1.50 ± 0.08	1.58 ± 0.12	1.34 ± 0.12	1.46	1.12
d_6/d_4	1.29 ± 0.06	1.34 ± 0.07	1.18 ± 0.09	1.29	1.06
d_6/d_3		1.76 ± 0.15	1.38 ± 0.15	1.62	1.21

in Table 7. The ABCLOS data clearly prefer the vector to scalar gluons. On the other hand, the CDHS data show that these results are very sensitive to even small corrections (in the CDHS Q^2 range one would expect Nachtmann moments to be practically equivalent to ordinary moments). Although there are some doubts about the significance of this test[39] it is fair to say that QCD predictions are in a good agreement with experimental data.

Another QCD prediction is that moments of xF_3 should fall with Q^2 as powers of $\log Q^2/\Lambda^2$ [Eq. (15)] or equivalently

$$(M_N^{xF_3})^{-1/d_N} \sim \log Q^2/\Lambda^2 .$$

As we see from Fig. 28, Nachtmann moments of ABCLOS and of CDHS are in good agreement with this prediction, yielding however different Λ's, see Table 8.

Table 8

Values of Λ from $\left[M_N^{xF_3}(Q^2) \right]^{-1/d_N} \sim (\log Q^2/\Lambda^2)$

Collaboration	Moments	Λ
ABCLOS [3]	Nachtmann	0.74 ± 0.05
CDHS [38]	Nachtmann	0.33 ± 0.15
	Ordinary	0.60 ± 0.15
ABCLOS [41]	Nachtmann	0.72 ± 0.13

From Fig. 24 one may get an impression that there is serious discrepancy between these two experiments: the scale is different by a factor of 2! This is mainly because d_N depends on the number of flavours assumed

$$d_N = \frac{4}{33 - 2f} \left[1 - \frac{2}{N(N+1)} + 4 \sum_{j=2}^{N} \frac{1}{j} \right] .$$

The choice of f = 3 by ABCLOS and f = 4 by CDHS amounts to 50% of the discrepancy. As shown by Wotschack[19], after taking into account some other minor differences in the analysis (treatment of quasi-elastic events, radiative corrections) one is left with $\sim 1\sigma$ discrepancy. Let us stress that this simple first order in α_s formula (15) describes very well data down to surprisingly low Q^2 of the order of 1 GeV^2! This agreement is even more surprising when we realize that, with Λ = 0.75, the value of $\alpha_S(Q^2)$ at Q^2 = 1.5 is close to 2!

The analysis of the moments for F_2 is a little bit more complicated, as they are coupled with moments of gluon distribution. One may write

$$YM_N^{F_2}(Q^2) = M_N^{F_2}(Q_0^2) + XM_N^G(Q_0^2) \ , \qquad (20)$$

where X and Y are known functions of Q^2 and Λ. The ABCLOS Collaboration[3] has fitted its data with Eq. (23) obtaining moments of gluon distribution at $Q_0^2 = 5$ GeV^2 (see Table 9). The first two moments can be compared with the values obtained by CDHS from a Buras-Gaemers-type analysis; agreement is good.

Second-order Corrections

The moments analysis has some weak points; for full discussion see Ref. 32. One of them is the question of second-order corrections. As we have already seen, a relatively large value of α_S at small Q^2 implies the need to worry about second-order corrections. In second order in α_S QCD predicts for non-singlet structure functions

$$M_N^{NS}(Q^2) = M_N^{NS}(Q_0^2)\left[\frac{\alpha_s(Q^2)}{\alpha_s(Q_0^2)}\right]^{d_N}\left\{1 - a^N\left[\alpha_s(Q^2) - \alpha_s(Q_0^2)\right]\right\} \ ,$$

$$(21)$$

where now

$$\alpha_s(Q^2) = \frac{12\pi}{(33 - 2f)\log(Q^2/\Lambda^2)}\left[1 - \frac{\beta_1}{\beta_0^2}\frac{\log\log(Q^2/\Lambda^2)}{\log(Q^2/\Lambda^2)}\right]$$

β_1, β_0 being known numbers. a^N is a set of numbers which can be calculated assuming some definition of coupling constant, or some definition of Λ. In other words the numbers a^N calculated using different renormalization prescription will give us different values of Λ. Therefore Λ has a meaning only if we specify the scheme used. In this situation there are two possibilities:

i) One may stick to some renormalization scheme yielding some set of numbers a^N; then fitting data with Eq. (21) one gets a value of Λ for this particular scheme. The most popular scheme is the so-called "minimal subtraction" scheme (MS). In this scheme second-order corrections reduce the value of Λ by approximately $\frac{1}{2}$, i.e.

$$\Lambda_{MS} \sim 0.5 \ \Lambda_{lowest\ order}[19,41] \quad .$$

ii) One may set all $a^N = 0$. This corresponds to different definitions of coupling constant for different N; the value of Λ should become N-dependent, with N-dependence calculable[42]. Figure 29 shows that lowest order [i.e. Eq. (15)] and second-order [i.e. Eq. (21) with $a_N = 0$] curves are almost identical, although they correspond to slightly different values of Λ. One may notice that second-order Λ_{ABCLOS} and Λ_{CDHS} are in better agreement than in the leading order case. Figure 30 shows that existing data are not precise enough to test QCD-predicted N-dependence of Λ, in particular the difference between Λ of ABCLOS and Λ of CDHS is bigger than the expected effect.
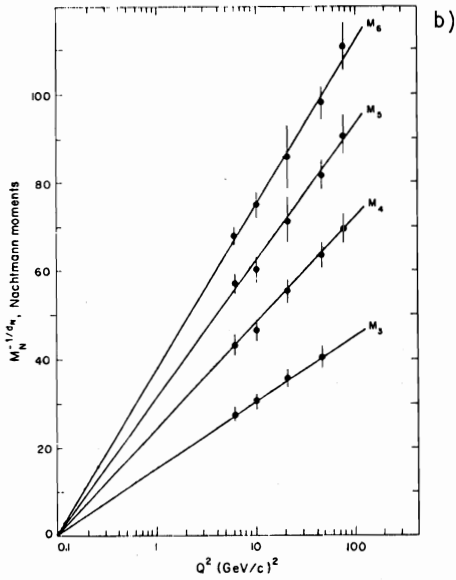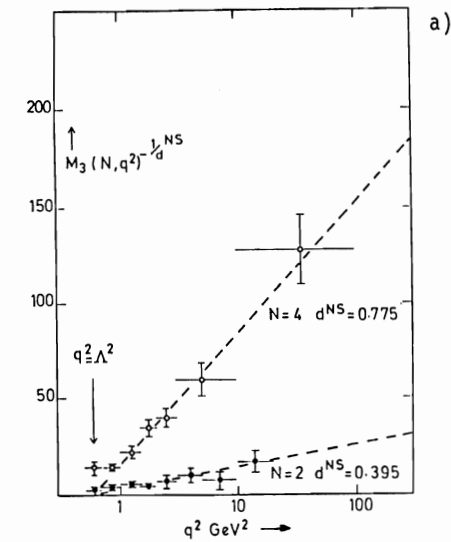

Fig. 28 Moments of xF_3 raised to $-1/d_N$ as a function of Q^2. a) ABCLOS, and b) CDHS.

Table 9

Gluon moments, $M_N^G(Q_0^2 = 5 \text{ GeV}^2)$

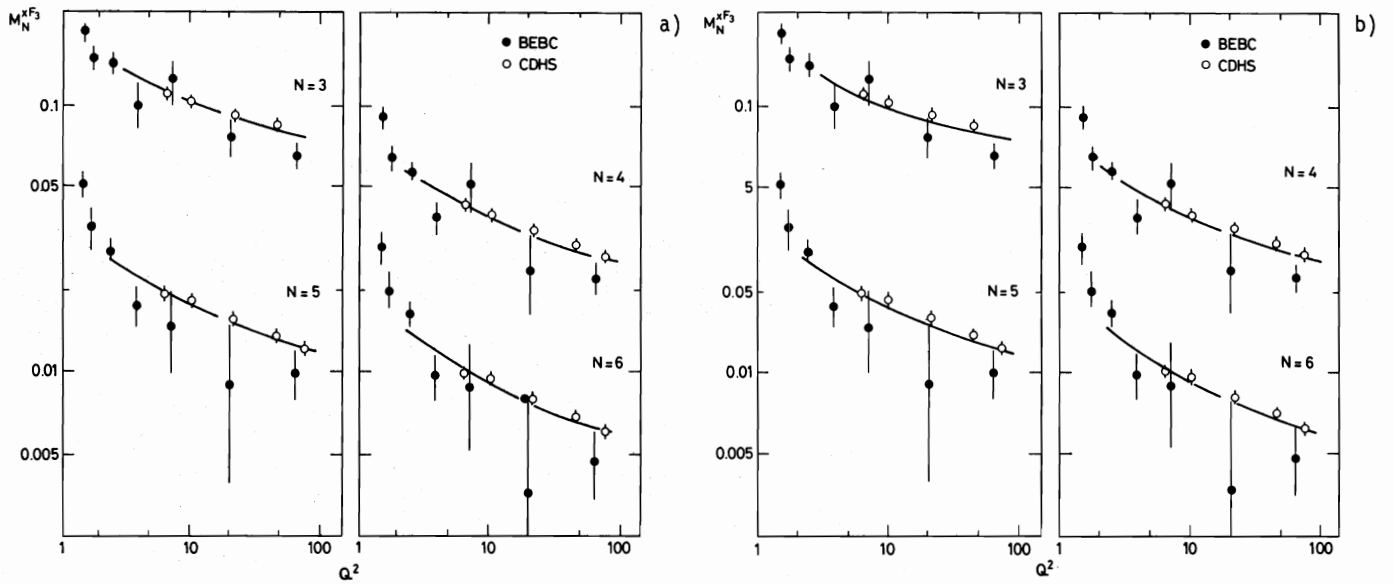| N	$M_N^G(5 \text{ GeV}^2)$	Q^2 range used
2	0.62 ± 0.15	1 – 20
3	0.12 ± 0.05	1 – 100
4	0.03 ± 0.02	1 – 100
5	0.02 ± 0.01	1 – 100

Fig. 29 a) Fit of the leading-order formula to a combined ABCLOS–CDHS data set ($Q^2 > 2$ GeV) assuming four flavours. The corresponding values of Λ are: $\Lambda_3 = 0.48 \pm 0.13$, $\Lambda_4 = 0.43 \pm 0.09$, $\Lambda_5 = 0.34 \pm 0.08$, $\Lambda_6 = 0.35 \pm 0.06$. b) Fit of the second-order formula to a combined ABCLOS–CDHS data set ($Q^2 > 2$ GeV) assuming four flavours. The corresponding values of Λ are: $\Lambda_3 = 0.53 \pm 0.11$, $\Lambda_4 = 0.43 \pm 0.07$, $\Lambda_5 = 0.43 \pm 0.08$, $\Lambda_6 = 0.45 \pm 0.08$.
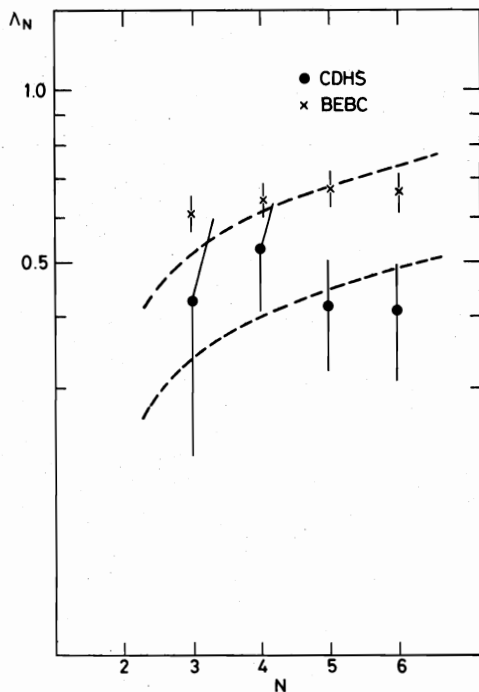
Conclusions

In the past few years considerable progress has been made in the measurements of nucleon structure functions with neutrinos. We have high-statistics, precise data covering the Q^2 range from ~ 1 to 100 GeV^2. The very interesting fact is that the so-called "naïve" quark-parton model provides a very good description of these data. Some small deviations are observed, however, especially in the low Q^2 region (let us remember that the QPM was designed for the "deep inelastic", i.e. large Q^2 and ν region). These deviations are very well described by lowest order predictions of QCD down to surprisingly low Q^2, with $\Lambda \approx 0.5$. More precise data, as well as more theoretical understanding, is needed however before we can announce that QCD is the true theory of strong interactions.

Fig. 30 Comparison of predicted and observed N-dependence of the parameter Λ obtained from fits of Eq. (24).

Acknowledgements

REFERENCES

1. M. Jonker et al., Phys. Lett. 86B, 229 (1979).

2. E. Fernandez et al., Study of the u and d̄ + s̄ quark distributions in the proton using anti-neutrino-proton scattering, paper submitted to the Neutrino '79 Conference, Bergen.

3. P.C. Bosetti et al., Nucl. Phys. B142, 1 (1979).

4. J.G.H. de Groot et al., Z. Phys. C 1, 143 (1979).

5. A. Benvenuti et al., Phys. Rev. Lett. 42, 1317 (1979).

6. H. Deden et al., Nucl. Phys. B85, 269 (1975).

7. J.P. Berge et al., Phys. Rev. Lett. 39, 382 (1977).

8. A. Benvenuti et al., Phys. Rev. Lett. 42, 149 (1979).

9. D. Sinclair et al., Measurement of x and y distributions for antineutrino charged current inelastic scattering, submitted to the Neutrino '79 Conference, Bergen.

10. H. Weerts et al., ABBLS Collaboration, First results from ν̄ charged-current interactions in Gargamelle at the SPS, presented at the Neutrino '79 Conference, Bergen.

11. J. Pilcher, Review of dimuon production in hadron collisions, these proceedings.

12. G. Altarelli, R.K. Ellis and G. Martinelli, MIT preprint CTP-776 (1979).

13. R. Stroynowski, to be published *in* Proc. Summer Institute on Particle Physics, Stanford, 1979.

14. A. Benvenutti et al., Phys. Rev. Lett. 41, 1204 (1978).

15. H.J. Willutzki, CDHS Collaboration, New results on opposite- and like-sign dimuon production, presented at the Neutrino '79 Conference, Bergen.

16. R. Feynmann, Photon-hadron interactions (Benjamin, New York, 1972).

17. B.C. Barish et al., Charged-current neutrino and antineutrino cross section results from the CITFR experiment, Fermilab. Conf. 78/46-Exp.

18. P. Musset and J.P. Vialle, Neutrino physics with Gargamelle, Phys. Reports 39C (1978).

19. A. Savoy-Navarro, Charged-current results from the CDHS experiment, presented at the Neutrino '79 Conference, Bergen.
    J. Wotschack, talk at the EPS Int. Conf. on High-Energy Physics, Geneva, 1979.

20. T. Kafka et al., High-energy charged current neutrino interactions in deuterium, submitted to this Symposium.

21. S.J. Barish et al., ANL-HEP-PR-78-30 (1978).

22. N.P. Samios, Proc. Int. Symposium on Lepton and Photon Interactions at High Energies, Stanford, 1975 (SLAC, Stanford, 1975), p. 527.

23. W. Lerche et al., Nucl. Phys. B142, 65 (1978).

24. J. Guy, Measurement of the ratio of the total charged-current cross-sections of high-energy neutrinos on neutrons and protons, presented at the Neutrino '79 Conference, Bergen.

25. O. Enriques et al., Phys. Lett. 80B, 309 (1979).

26. V.I. Efremenko et al., Phys. Lett. 84B, 511 (1979).

27. M. Jonker et al., First results from the CERN-Hamburg-Amsterdam-Rome-Moscow neutrino experiments, presented at EPS Int. Conf. on High-Energy Physics, Geneva, 1979.

28. H.C. Ballagh et al., Phys. Lett. 79B, 320 (1978).

29. H. Deden et al., Nucl. Phys. B85, 269 (1975).

30. E.M. Riorden et al., SLAC Pub. 1634 (1975).

31. G. Altarelli and G. Parisi, Nucl. Phys. B126, 298 (1977).

32. J. Ellis, Invited talk at Neutrino '79 Conference, Bergen, Preprint TH 2701-CERN (1979).

33. O. Nachtmann, Nucl. Phys. B63, 237 (1973) and B78, 455 (1977).

34. A. Buras and K.J.F. Gaemers, Nucl. Phys. B132, 249, (1978).

35. J.G.H. de Groot et al., Phys. Lett. 82B, 456 (1979).

36. W. Furmanski and S. Pokorski, Preprint TH 2685-CERN (1979).

37. L. Baulieu and C. Kounnas, Nucl. Phys. B155, 429 (1979).

38. J.G.H. de Groot et al., Phys. Lett. 82B, 292 (1979).

39. H. Harari, SLAC PUB-2254 (1979).

40. R. Barbieri, L. Caneschi, G. Curci and D. d'Emilio, Phys. Lett. 81B, 207 (1979).

41. J.G. Morfin, ABCLOS Collaboration, Comparison of structure functions from the BEBC-GGM data with QCD predictions, presented at Neutrino' 79 Conference, Bergen.

42. A. Para and C. Sachrajda, Phys. Lett. 86B, 337 (1979). See also D.W. Duke and R.C. Roberts, Rutherford Lab. preprints RL-79-025 and RL-79-044 (1979).

DISCUSSION

Tom Kirk (FNAL): You showed some plots from four different groups of $F_2(x)$, which is finally the experimentally measured quantity and you said that you saw some slight inconsistencies but you quoted no statistical test for mutual compatibility. It seemed to me even from the back row that those were grossly incompatible with one another. That is a comment. The question I have is: if you examine the data carefully, is it that they are truly mutually incompatible or has the analysis been done in different ways such that they appear to be mutually incompatible but are not?

Para: The biggest difference is between F_2 of ACMP and the other groups, which I think is due to physics. As far as the remaining three groups are concerned, the analysis is done in a very similar way. The differences in the treatment of the radiative corrections or the corrections for Fermi motion do not explain the existing discrepancies which, in my opinion, are not very big.

Orin Fackler (Rockefeller): The genesis of my question is similar to the one Tom just asked. Could you quantify for us the experimental x resolution that is inherent in the CDHS apparatus and how it affects the measured structure functions?

Para: The x resolution depends very much on Q^2. At high Q^2, let us say 50 GeV, $\Delta x/x$ is of the order of 20%. At $Q^2 = 5$ GeV $\Delta x/x$ rises from $\sim 25\%$ at low x to $\sim 40\%$ at x around 0.5. The structure functions were corrected for these effects. Points for which corrections were bigger than 25% were not used in the analysis.

Fackler: I noticed that in xF_3 you go down to 10^{-3} in x. Somewhere in that region, at very small x, I should think that the effects of resolution would become very large.

Para: The very small x region gives a significant contribution to the Gross-Llewellyn-Smith integral. As a lower integration limit CDHS has chosen $x_0 = 5 \times 10^{-3}$, which I think is still reasonable.

Herbert Anderson (Enrico Fermi Institute, Chicago): When you use the Altarelli-Parisi equations, that requires an integral from x to 1, where do you get the data in the region x large and close to 1?

Para: One usually extrapolates measured structure functions towards x = 1 using some polynomials.

Anderson: Do you not still have the same problems that you get up there with the higher twist corrections and resonances?

Para: Smooth extrapolation towards x = 1 is the best one can do. The question can be raised: What is the meaning of the results obtained this way. There is some hope that smooth extrapolation averages over resonance peaks somehow taking them into account. Higher twist effects are quite far from being understood. All this was discussed in details by J. Ellis in his talk at the Bergen Conference.

A. Bodek (Rochester): I have an experimental question. We saw from Strovink's talk that comparing his muon data with the SLAC data and the CDHS data with the SLAC data he claimed that both the CDHS data and the muon data have an 18% discrepancy from the SLAC data when he compares them in the same ν region. On the other hand you claim that the SLAC data and the CDHS data are consistent. Is this statement only correct at 20%?

Para: From Fig. 24 you see that the SLAC points lie very well within the error bars at the CDHS points. I do not think you can claim any inconsistency. I propose to wait for the talk of Bill Williams, who will present a quantitative comparison of muon, electron and neutrino data.